Dynamics of Enhanced Tracer Diffusion in Suspensions of Swimming Eukaryotic Microorganisms

Kyriacos C. Leptos[1], Jeffrey S. Guasto[2], J.P. Gollub[1,2], Adriana I. Pesci[1], and Raymond E. Goldstein[1]
[1]*Department of Applied Mathematics and Theoretical Physics, University of Cambridge, Wilberforce Road, Cambridge CB3 0WA, UK and*
[2]*Department of Physics, Haverford College, Haverford, PA 19041*
(Dated: October 19, 2009)

In contexts such as suspension feeding in marine ecologies there is an interplay between Brownian motion of non-motile particles and their advection by flows from swimming microorganisms. As a laboratory realization, we study passive tracers in suspensions of eukaryotic swimmers, the alga *Chlamydomonas reinhardtii*. While the cells behave ballistically over short intervals, the tracers behave diffusively, with a time-dependent but self-similar probability distribution function of displacements consisting of a Gaussian core and robust exponential tails. We emphasize the role of flagellar beating in creating oscillatory flows that exceed Brownian motion far from each swimmer.

PACS numbers: 87.17.Jj, 05.40.-a, 47.63.Gd, 87.23.-n

For many of the microscopic organisms in marine and lake environments the process of feeding involves an interplay between diffusion of target particles and their advection in the flow field of the swimmers [1–4]. For particles large enough to have negligible Brownian motion the rate of interception is determined primarily by their size and details of fluid streamlines around the swimmers, while for molecular species the uptake rate depends on boundary layers characteristic of high Péclet number flows [3, 5]. As the concentration of swimmers increases, the greater frequency of encounter of suspended particles with the swimmer flow fields will inevitably lead to enhanced transport of the particles themselves.

At high *swimmer* concentrations there is now ample evidence from bacterial systems [6] that collective behavior can emerge, consisting of large-scale vortices and jets which dramatically enhance tracer particle transport and fluid mixing. Despite significant progress in understanding collective behavior of swimmers [7, 8], the fundamental problem of understanding enhanced tracer diffusion induced by microorganisms has remained largely unsolved, even in the dilute swimmer limit in which interactions between the organisms are negligible.

One appealing point of view [6, 9] is that the sea of swimming organisms constitutes an effective"thermal bath," analogous to the multitudes of molecules responsible for Brownian motion, where each encounter of a tracer particle with a swimmer provides a random kick. In conventional Brownian motion, *e.g.* with micron-size particles in water, there is an enormous separation of time scales between the duration of molecular collisions (ps) and the observed particle motion (ms). In contrast, in a suspension of microorganisms it is possible to resolve the encounters with tracer particles, and the dynamical problem involves correlated *advective trajectories* in the presence of true Brownian noise. This problem is reminiscent of passive scalar advection in turbulent flows [10], where the probability distribution functions (PDFs) of tracer displacements become strongly non-Gaussian.

Here we report an advance in the study of tracer statistics in suspensions of swimmers. First, we use the alga *Chlamydomonas reinhardtii* [11], a biflagellated model eukaryote in the study of photosynthesis and flagella. Relative to the bacteria studied previously [6] (*E. coli*, *B. subtilis*) *Chlamydomonas* has features that will greatly simplify the theoretical interpretation of our results; it is nearly spherical, is sufficiently large (a radius $R \sim 5$ μm) that it is not subject to substantial rotational diffusion, and as its two $10 - 12$ μm long flagella beat in a synchronized "breast stroke" pattern at ~ 50 Hz, it displays long periods of nearly straight-line motion (up to ~ 10 s [12]). Second, we characterize in detail the time-dependent PDF of tracer displacements, and find clear systematic deviations from Gaussianity, in the form of an exponential tail whose amplitude grows with swimmer concentration. Despite this complex form, the PDFs exhibit self-similarity under a diffusive scaling. Some physical considerations that may be important in a theory of these results are suggested.

Microscopy of *Chlamydomonas* suspensions was carried out on a Nikon TE2000-U inverted fluorescence microscope inside disk-shaped chambers fabricated from polydimethylsiloxane (PDMS), 1 cm in diameter and 1.5 mm deep. After casting, each cavity was etched in an oxygen plasma (Femto, Diener Electronic) and bonded to a PDMS-spin-coated cover slip. Both the interior of the chambers and the fluorescent particles were pacified using a 5% (w/v) solution of bovine serum albumin to prevent the protein in the flagella from adhering to them [13]. *Chlamydomonas reinhardtii* (UTEX 89) was grown axenically in Tris-Acetate-Phosphate (TAP) medium [11], on an orbital shaker (300 rpm) in a diurnal growth chamber (KBW400, Binder). The daily cycle was 16 h of cool white light ($\sim$ 80 μmol photons/m^{2}s PAR) at 28 °C, and 8 h in the dark at 26 °C. For concentrations $> 10^6$ cells/cm^3, cells were concentrated from

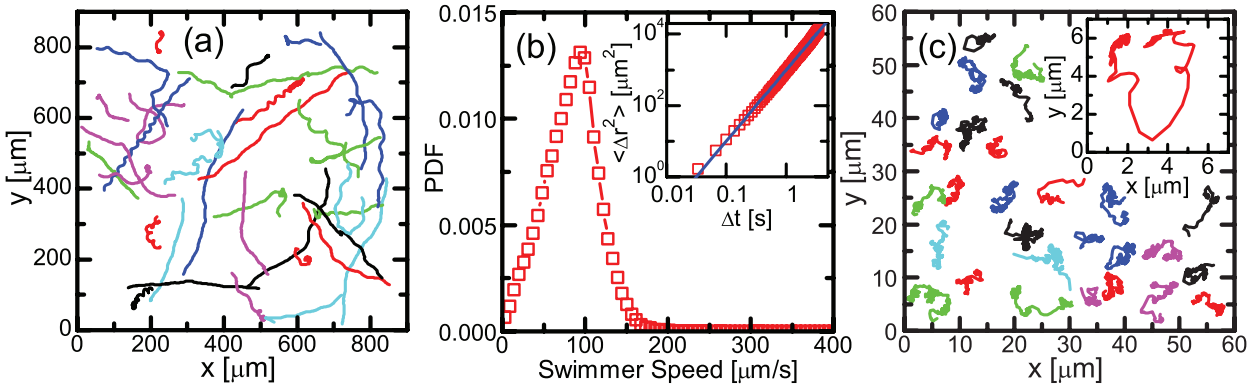

FIG. 1: (Color online) Swimming cells and tracer particles. (a) *Chlamydomonas* trajectories over an interval of $\sim$ 1s. (b) PDF of swimming speed obtained at 30 fps, averaged over 30 s, and (inset) mean squared displacement of swimmers in the imaging plane. The line $\langle \Delta r^2 \rangle \sim t^2$ shows the motion to be ballistic for intervals up to several s. (c) Trajectories of 2.0 μm microspheres observed at 50 fps. Inset: loopy tracer path, sampled at 500 fps, induced by a cell passing within ~ 8 μm.

exponentially growing cultures by centrifugation in tubes at $1100 \times g$ and addition of fresh TAP to the cell pellet. The tubes were then placed in the diurnal chamber for at least 1 h to allow the cells to recuperate. All cell concentrations were measured using a haemocytometer [14]. Fluorescent microspheres (yellow-green, Invitrogen F8827; radius $a = 1$ μm,) were added to obtain a final concentration of $\sim$ 250 ppm (w/v). Each sample was transferred to a separate PDMS observation chamber, taking care to avoid excessive shear that might damage the flagella. Movies of cells and of tracer particles were recorded with a high-speed video camera (Fastcam SA-3, Photron) at up to 500 fps to resolve motion induced by flagellar beating. Tracers were observed at $\times$40 (NA 0.6) with epifluorescence illumination (Pantachrome, Till Photonics) in a plane ~ 100 μm above the chamber bottom. Cell and particle paths were extracted from recordings with a predictive particle tracking algorithm [15].

A relatively dilute suspension of cells (5×10^6 cm^{-3}) in growth medium was first studied at $\times$20 magnification (NA 0.45) with bright-field illumination, using a red long-pass filter ($\lambda > 620$ nm) to prevent phototaxis. While cell trajectories have been studied previously [12, 16], it is important to characterize them *in situ* along with the tracer dynamics. The representative sample in Fig. 1a illustrates a broad spectrum of trajectories including helical paths of variable pitch – the well-known spinning of the body around the trajectory midline [11]. The cell speed distribution in the imaging plane (Fig. 1b) shows a peak at ~ 100 μm/s. There is some out-of-plane motion that is not imaged, so the 3D distribution may be even sharper. The distribution is consistent with swimming at approximately constant speed in random directions. Indeed, while many trajectories' centerlines are gently curved, sharp turns are only observed for $\Delta t > 10$ s [12]. A statistical analysis of cell displacements along an arbitrary axis in the imaging plane shows *ballistic* behavior (Fig. 1b, inset) up to several seconds. Tracer trajectories (Fig. 1c and inset) involve both Brownian components and large jumps induced by flows from the swimmers. Higher magnification (inset) shows that these advective motions are loops due to flagellar beating.

For each volume fraction ϕ of *Chlamydomonas* the PDF of tracer displacements $P(\Delta x, \Delta t)$ along an arbitrary direction was calculated for a number of increasing time intervals Δt. The intervals used were well within the ballistic regime of the swimmers (Fig. 1b), and an order of magnitude smaller than the mean time between sharp turns measured in three-dimensional tracking experiments [12]. Figure 2a shows the PDF at a fixed interval ($\Delta t = 0.12$ s) for increasing ϕ. Without swimmers, the distribution is accurately fitted by a Gaussian whose width is determined by the diffusion constant $D_0 = 0.28$ μm^2/s, consistent with the Stokes-Einstein value.

In the presence of swimmers, there are two changes to the distributions. First, exponential tails appear in the PDFs, the magnitudes of which grow with increasing concentration of swimmers. Second, the Gaussian core broadens significantly. For all volume fractions ϕ and time intervals Δt the distributions $P(\Delta x, \Delta t)$ can be fitted approximately (in $\log(P)$, using a nonlinear least squares algorithm) to a weighted sum of Gaussian and exponential (Laplace) distributions,

$$P(\Delta x, \Delta t) = \frac{1-f}{(2\pi\delta_g^2)^{1/2}} \mathrm{e}^{-(\Delta x)^2/2\delta_g^2} + \frac{f}{2\delta_e} \mathrm{e}^{-|\Delta x|/\delta_e} \ . \quad (1)$$

The mean absolute deviation between the fit and the data for $\log(P)$ is ~ 0.1, corresponding to 3% of the range of $\log(P)$ shown in the data. There are three parameters: the standard deviation $\delta_g(\Delta t, \phi)$ of the Gaussian distribution, the decay length $\delta_e(\Delta t, \phi)$ of the Laplace distribution, and the fractional contribution $f(\phi)$ of advection-enhanced displacements. We find that both lengths exhibit diffusive growth, with $\delta_g \simeq A_g \Delta t^{1/2}$ and $\delta_e \simeq$

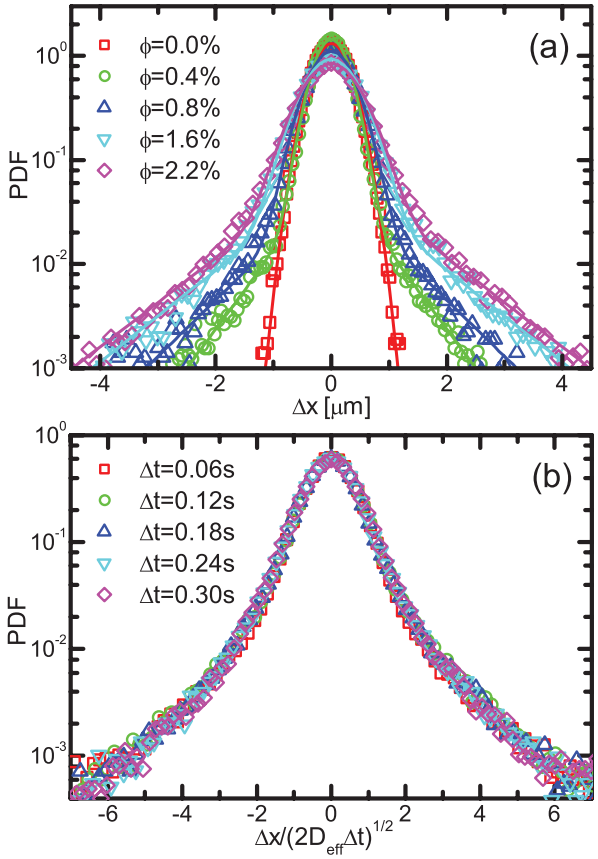

FIG. 2: (Color online) Probability distribution functions for tracer displacements. (a) Overlaid PDFs at a fixed time interval $\Delta t = 0.12$ s, for various volume fractions, showing the broadening of the Gaussian core and appearance of exponential tails. (b) Diffusive rescaling of PDFs at $\phi = 2.2\%$ and various time intervals, illustrating data collapse.

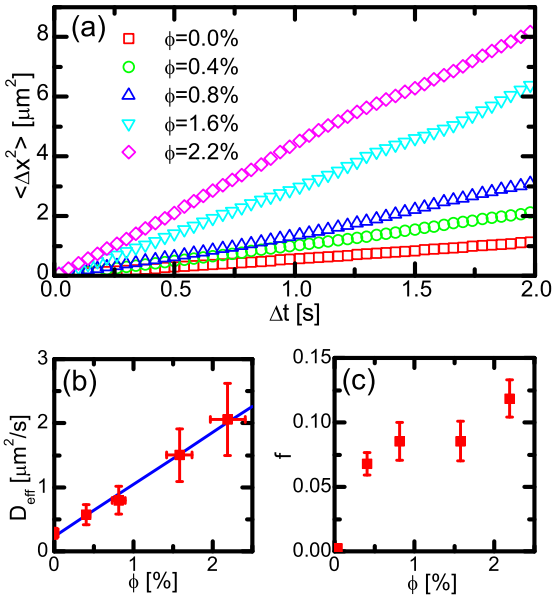

FIG. 3: (Color online) Diffusional properties. (a) Mean squared tracer displacement at various cell concentrations. Concentration dependence of (b) effective diffusivity, with linear fit, and (c) fractional contribution of PDF tails.

$A_e \Delta t^{1/2}$. This implies that a diffusive rescaling of the displacements in terms of $\Delta x/(2D_{\rm eff}\Delta t)^{1/2}$ leads, at any given ϕ, to a data collapse, as shown in Fig. 2b, where $D_{\rm eff}$ is a constant (see below). Furthermore, despite the complex shape of the PDFs, the mean square displacement of the tracers remains linear in time, with a slope that increases with ϕ (Fig. 3a), apart from small variations from run to run that are not statistically significant. Similar trends have been seen in thin films of swimming bacteria [6]. We characterize this behavior by means of an effective diffusivity $D_{\rm eff} = \langle(\Delta x)^2\rangle/2\Delta t$, and find that $D_{\rm eff}$ increases with the volume fraction of swimmers with a form $D_{\rm eff} \simeq D_0 + \alpha\phi$ [8], with $D_0 = 0.23$ μm^2/s and $\alpha = 81.3$ μm^2/s ($R^2 = 0.99$) (Fig. 3b). Although there is not yet a microscopic theory of this diffusional enhancement, on dimensional grounds we expect $\alpha \sim U^2\tau \sim U\ell$, where U, τ, and ℓ are: a characteristic advective velocity, encounter time, and advected length. These can be estimated various ways; perhaps the simplest is to note that because the measurement time scale encompasses several to many beat periods, ℓ represents a *net* displacement. The inset to Fig. 1c illustrates that a typical ℓ might be $1-3$ μm (as measured by the track end-to-end distance), which implies a velocity $U \sim 30-80$ μm/s, a value that is sensibly within the cell speed distribution (Fig. 1b). The value of f increases (from zero) with ϕ (Fig. 3c), and dimensional analysis suggests we may infer an effective range over which advective displacements are substantial as $R_{\rm eff} \sim R(f/\phi)^{1/3} \simeq 10.3$ μm (using the mean of individual measurements of f in Fig. 3c).

These measurements suggest a heuristic picture of the suspension; surrounding each cell is a *sphere of influence* of radius $R_{\rm eff}$ within which advection *strongly* dominates diffusion, and outside of which tracers experience only effective Brownian motion. This is consistent with the PDFs having the form of a weighted sum of the two distributions. $R_{\rm eff}$ and f provide measures of this sphere size; at the highest concentration ($\phi = 2.2\%$, $f \simeq 0.12$) the mean distance between spheres is ~ 30 μm, almost thrice $R_{\rm eff}$, so binary interactions are negligible.

A quantitative measure of the advection/diffusion balance comes from considering the flow field around a cell in the simplified form $u(r)\exp(i\omega t)$. Tracer oscillations are indistinguishable from Brownian motion at a radius $r_B > R_{\rm eff}$ where the displacement $2u(r_B)/\omega$ in a half cycle is comparable to the diffusive displacement $(2Dt)^{1/2}$ in a time $t = \pi/\omega$. For *Chlamydomonas* flagellar beating

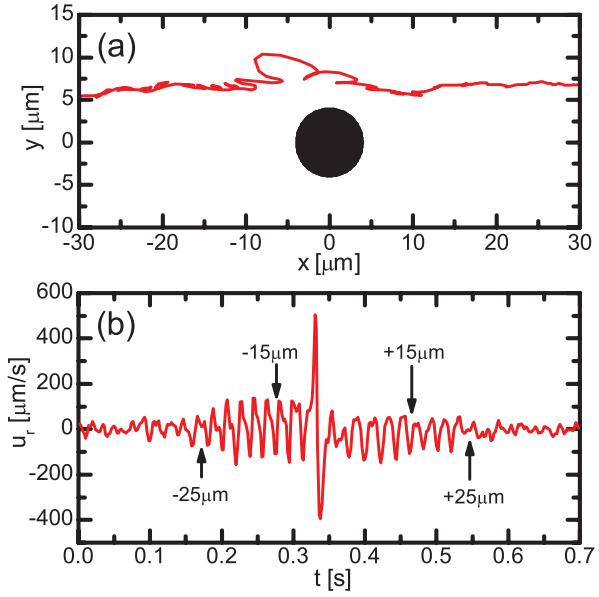

FIG. 4: (Color online) Tracer dynamics. (a) Trajectory of a tracer particle imaged at 500 fps, in a frame of reference moving with a *Chlamydomonas* cell. Black disk represents the approximate size of the cell. (b) Induced radial motion fades into Brownian motion beyond ~ 25 μm from the cell.

with $\omega = 2\pi \cdot 50$ rad/s this yields $u(r_B) \sim (2\pi D\omega)^{1/2} \sim 10$ μm/s, and a displacement ~ 0.1 μm. A direct experimental determination of r_B can be obtained from simultaneous bright-field microscopy of tracer motion and free-swimming cells. Figure 4a shows one such trajectory, under the same conditions as in Figs. 1c, 2, and 3, plotted in the frame of reference of the swimming *Chlamydomonas*, along with the time series of radial velocity in the laboratory frame (Fig. 4b). Inspection of Fig. 4b suggests the estimate $r_B \simeq 25 - 30$ μm. For comparison one might ask when oscillatory displacements are comparable to the tracer radius, $2u(r_a)/\omega \simeq a$, which yields $u(r_a) \sim 150$ μm/s. Such velocities appear at distances of order 15 μm ($\sim 1.5R_{\rm eff}$). To go beyond these measurements to a model for the velocity field we note that the viscous penetration depth associated with the flagellar beating is $\xi = (2\nu/\omega)^{1/2} \simeq 80$ μm. This is only a few times larger than r_B so these flows are intrinsically *unsteady*. Detailed comparison [17] with tracer trajectories shows quantitative consistency with such models and confirms the length scale r_B. Moreover, the number of flagellar beats during the intervals Δt of the PDFs, and also during the encounter time of a tracer with a swimmer, can easily be ten or more. Such unsteadiness may alter significantly encounter rates in suspension feeding relative to those for steady flow [2, 3]. It also contributes to an enhanced tracer diffusivity, as in the problem of pollutant dispersal in oscillatory tidal flows [18].

We have shown that the statistics of passive tracers in suspensions of flagellated eukaryotes exhibits a non-Gaussian yet self-similar form, with clear systematics in the concentration of swimmers. Oscillatory components appear to play a significant role in the dynamics. Development of a statistical theory of the PDFs and the diffusional enhancement is clearly the outstanding theoretical challenge. In closing, we note that in contrast to bacteria, whose helical flagella push it through the fluid, *Chlamydomonas* is a "puller." Theoretical studies of instabilities in concentrated suspensions of swimmers [7] suggest a profound difference between the two, with only pushers displaying large-scale coherence. The techniques outlined here may allow for sufficiently high concentrations of cells to test this prediction in detail.

We thank K. Drescher, B. Eckhardt, T.J. Pedley, and C.A. Solari for discussions, and N. Damean, D. Page-Croft and N. Price for technical assistance. Work supported by the BBSRC, a Leverhulme Trust Visiting Professorship (JPG), NSF Grant DMR0803153 (JSG & JPG), and the Schlumberger Chair Fund. JPG appreciates the hospitality of DAMTP during this work.

[1] J. Shimeta, Limnol. Oceanogr. **38**, 456 (1993).
[2] S. Mayer, Bull. Math. Biol. **62**, 1035 (2000).
[3] V.J. Langlois, *et al.*, Aquat. Microb. Ecol. **54**, 35 (2009).
[4] S. Humphries, Proc. Natl. Acad. Sci. USA **106**, 7882 (2009).
[5] V. Magar, T. Goto, and T.J. Pedley, Q. J. Mech. Appl. Math. **56**, 65 (2003); M.B. Short, *et al.*, Proc. Natl. Acad. Sci. USA **103**, 8315 (2006).
[6] X.-L. Wu and A. Libchaber, Phys. Rev. Lett. **84**, 3017 (2000); C. Dombrowski, *et al.*, Phys. Rev. Lett. **93**, 098103 (2004).
[7] J.P. Hernandez-Ortiz, C.G. Stoltz, and M.D. Graham, Phys. Rev. Lett. **95**, 204501 (2005); D. Saintillan and M.J. Shelley, Phys. Fluids **20**, 123304 (2008).
[8] P.T.Underhill, J.P. Hernandez-Ortiz, and M.D. Graham, Phys. Rev. Lett. **100**, 248101 (2008).
[9] L. Angelani, R. Di Leonardo, and G. Ruocco, Phys. Rev. Lett. **102**, 048104 (2009).
[10] Z. Warhaft, Annu. Rev. Fluid Mech. **32**, 203 (2000), and references therein. See also P. Chaudhuri, L. Berthier, and W. Kob, Phys. Rev. Lett. **99**, 060604 (2007).
[11] E.H. Harris, *The Chlamydomonas Sourcebook*, Vol. 1 (Academic Press, Oxford, 2009).
[12] M. Polin, *et al.*, Science **325**, 487 (2009).
[13] D.B. Weibel *et al.*, Proc. Natl. Acad. Sci. USA **102**, 11963 (2005).
[14] Concentrations were corrected for phototaxis effects from epifluorescent illumination using a calibration based on microsphere diffusivity obtained from bright-field illumination with no phototaxis.
[15] N.T. Ouellette, H. Xu, and E. Bodenschatz, Exp. Fluids **40**, 301 (2006).
[16] V.A. Vladimirov, *et al.*, J. Exp. Biol. **207**, 1203 (2004).
[17] A.I. Pesci, *et al.*, unpublished (2009).
[18] M.S. Krol, SIAM J. Appl. Math. **51**, 1622 (1991).